# Observed Effects of Interparticle Friction and Particle Size on Shear Behavior of Granular Materials

Bei Bing Dai[1]; Jun Yang, F.ASCE[2]; and Cui Ying Zhou[3]

**Abstract:** This paper presents an experimental study on the shear behavior of granular materials, focusing on the effects of interparticle friction and particle size, which are of fundamental importance but are not yet well understood. The experimental program consisted of a large number of direct shear tests on glass beads of varying sizes and interparticle friction conditions, performed under a range of packing densities and normal stress levels. Test data were interpreted in terms of the stress–dilatancy relationship and shear strength parameters. The study indicates that under otherwise similar testing conditions, oil-lubricated glass beads tend to have substantially lower shear strength as compared with water-lubricated, water-flooded, and dry glass beads. It has also been found that at similar particle size uniformity, increasing mean particle size ($d_{50}$) leads to more dilatant shear response and higher shear strength. A generalized stress–dilatancy relation is proposed, which introduces a variable dilatancy coefficient that reflects on the effects of interparticle friction and particle size. It is shown that classical stress–dilatancy relations can be regarded as special cases of this generalized case, with the dilatancy coefficient being taken as a constant. Further explanations for the observed effects on macroscopic behavior are provided from the micromechanics perspectives.
**DOI: 10.1061/(ASCE)GM.1943-5622.0000520.** 

**Author keywords:** Shear behavior; Granular material; Interparticle friction; Particle size; Friction angle; Dilation angle; Stress–dilatancy relation.



## Introduction

The overall mechanical behavior of granular materials is complicated, highly dependent on the confining stress, packing density, and deformation pattern, as well as the characteristics of constituent particles, such as particle shape and size (e.g., Cavarretta et al. 2010; Yang and Wei 2012; Mahmud Sazzad et al. 2012; Li and Yu 2013). It has been of longstanding interest to investigate the relationship between the basic attributes of the individual particles and their macroscopic behavior. One of the most fundamental issues is the effect of interparticle friction on the overall shear resistance. As shown in Fig. 1, the theoretical predictions made by Bishop (1954), Caquot (1934), and Horne (1969) all suggested that the overall angle of shearing resistance of granular soils at the constant-volume condition, $\phi_{cv}$, also known as the critical-state friction angle, $\phi_{cs}$, increased with the interparticle friction angle, $\phi_\mu$. On the other hand, the laboratory direct-shear tests of Skinner (1969) suggested that $\phi_{cv}$ was not dependent on $\phi_\mu$. In recent years, numerical studies using the discrete-element method (Oger et al. 1998; Thornton 2000; Suiker and Fleck 2004; Kruyt and Rothenburg 2006; Maeda et al. 2006) showed that the constant-volume friction angle increased with the interparticle friction only in the range of low interparticle friction angles (i.e., $\phi_\mu$ ranges from 0 to about 15°), whereas in the range of relatively large interparticle friction (between about 15° and 40°) the constant-volume friction angle was not sensitive to a change of $\phi_\mu$. For the special case of $\phi_\mu = 0°$, the numerical simulations of Suiker and Fleck (2004) and Thornton (2000) indicated that the constant-volume friction angle approached zero, but the simulations of Kruyt and Rothenburg (2006), Maeda et al. (2006), and Oger et al. (1998) gave nonzero values of $\phi_{cv}$.

Another fundamental issue in relation to the shear strength of granular materials is the effect of particle size. The laboratory tests of Marachi et al. (1972) on rockfill materials showed that the angle of shearing resistance decreased with increasing mean particle size of the test materials. However, Al-Hussaini (1983), using triaxial compression and plane-strain tests on crushed basalt, showed that an increase of mean particle size resulted in an increase in the overall friction angle; similar observations were also reported by Hamidi et al. (2012).

Evidently, the influence of interparticle friction and particle size on the overall shear behavior of granular materials remains an open question. Given its fundamental importance and practical interest, an experimental study was carried out to address this question through a specifically designed laboratory testing program. The experimental program consisted of a large number of direct shear tests on glass beads of varying sizes and levels of interparticle friction, conducted under a range of packing densities and normal stress levels. In the following sections, the main results are presented and interpreted, leading to a generalized stress–dilatancy relation that accounts for the influence of interparticle friction and particle size.

## Testing Program and Data Interpretation

A total of 96 direct shear tests were performed under various testing conditions (Dai 2010). The apparatus used was an

[1]Assistant Professor, Research Institute of Geotechnical Engineering and Information Technology, School of Engineering, Sun Yat-sen Univ., Guangzhou 510275, China (corresponding author). E-mail: beibing_dai@yahoo.com

[2]Associate Professor, Dept. of Civil Engineering, Univ. of Hong Kong, Hong Kong, China; Distinguished Visiting Professor, Shanghai Jiao Tong Univ., Shanghai, China. E-mail: junyang@hku.hk

[3]Professor, Research Institute of Geotechnical Engineering and Information Technology, School of Engineering, Sun Yat-sen Univ., Guangzhou 510275, China. E-mail: zhoucy@mail.sysu.edu.cn

Note. This manuscript was submitted on August 28, 2014; approved on March 12, 2015; published online on April 25, 2015. Discussion period open until September 25, 2015; separate discussions must be submitted for individual papers. This paper is part of the ***International Journal of Geomechanics***, © ASCE, ISSN 1532-3641/04015011(11)/$25.00.

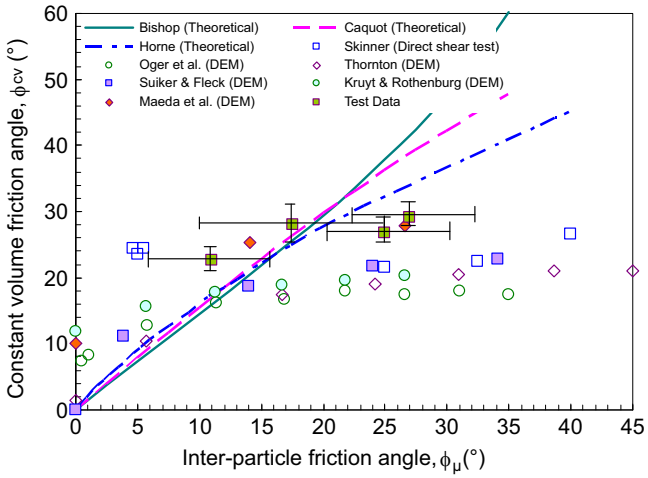


**Fig. 1.** Relations of the constant-volume friction angle $\phi_{cv}$ with the interparticle friction angle $\phi_{\mu}$

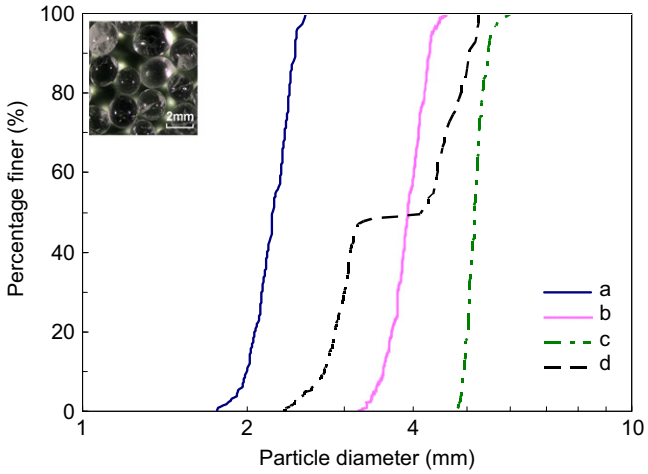


**Fig. 2.** Particle-size distribution curves of the glass beads tested

automatic strain-controlled direct shear machine, with a shear box of 100 × 100 × 36.5 mm. Despite several limitations, such as the nonuniform distribution of shear strains and shear stresses that have long been recognized (Shibuya et al. 1997), the direct shear test remains one of the most commonly used means to investigate the shear behavior and shear strength of soils in the laboratory. Granular materials used in the testing program were glass beads of different sizes; the simple and spherical geometry of glass beads allows the influence of particle shape (Yang and Wei 2012; O'Sullivan et al. 2002) to be isolated. Fig. 2 shows the particle gradation curves of the test materials, three of which were uniformly graded, with particle diameters ranging from 1.7 to 2.4 mm, 3.2 to 4.6 mm, and 4.8 to 6.0 mm, respectively. The fourth type of particle gradation was obtained by mixing two batches of glass beads with the sizes of 2.3–3.4 mm and 4.0–5.3 mm. In this paper, the four types of particle gradations are referred to as Gradations a ($d_{50}$ = 2.22 mm), b ($d_{50}$ = 3.90 mm), c ($d_{50}$ = 5.17 mm), and d (gap gradation), where $d_{50}$ = mean particle size; the uniformity coefficients for the Gradation Curves a, b, and c were determined to be 1.16, 1.14, and 1.06, respectively. The first three grading types have similar values of the coefficient of uniformity, allowing the uniformity coefficient's influence to be isolated when studying the effect of particle size. The use of Gradation d (gap gradation) was intended to further validate the investigation of the effect of interparticle friction. The uniformity coefficient, in fact, may exert an ineligible effect on the shear behavior of granular soil. This fascinating issue has been well recognized and investigated by other researchers, such as Oztoprak and Bolton (2013) and Ogbonnaya et al. (2009). This issue, however, is beyond the current research scope because this paper focuses on the effect of the interparticle friction and particle size. The ratio between the shear box height and the maximum particle size satisfied the requirements of ASTM standards for direct shear tests.

Four types of interparticle friction conditions were created in the testing program: (i) glass beads in a dry state (referred to as Friction Condition I), (ii) glass beads lubricated by water (referred to as Friction Condition II), (iii) glass beads flooded/submerged in water (Friction Condition III), and (iv) glass beads lubricated by edible oil (Friction Condition IV). Friction Conditions II and III, to some degree, can be alternatively interpreted as the unsaturated and saturated states, but they are not rigorously the same. Friction Conditions I and III were also examined in the direct shear tests of Skinner (1969), but those tests were conducted on monosized glass beads (1 and 3 mm, respectively). In creating Friction Condition II, glass beads were dipped into clean water so that they were well lubricated and were then taken out for subsequent testing. The lubrication might introduce capillary forces that make the interparticle friction slightly larger than that of water-submerged glass beads (Gabrieli et al. 2012). However, it has been found that such suction is insignificant for coarse granular soils (Jaafar and Likos 2011; Soria-Hoyo et al. 2009). For instance, Jaafar and Likos (2011) found that the matric suction in partially saturated glass beads decreased sharply with an increase of particle size: the measured suction for the case of particle size ranging from 0.032 to 0.045 mm was between 20 and 60 kPa, but it reduced to as low as 3 kPa for the case of particle size ranging from 0.25 to 0.3 mm. Given that the minimum size of the glass beads used in the present study is much greater than 1 mm, the effect of suction on the overall shear behavior is considered negligible.

The direct shear tests were performed under three normal stress levels, i.e., 19.6, 49.0, and 78.4 kPa, referred to as Stress Levels 1, 2, and 3, respectively. No particle crushing was observed in the test because the load level was far lower than the splitting strength of glass beads (Cavarretta et al. 2010). For all tests, a very low loading rate (0.1–0.2 mm/min) was used and therefore no excess pore-water pressure would be generated in cases involving glass beads submerged in water. The initial void ratios of all specimens fell into the range between 0.44 and 0.69. The loose specimens were reconstituted by deposition with gentle compaction at the top of the final specimen, and their void ratios are above 0.55. The dense specimens are prepared by layered deposition and compaction, and their void ratios are mostly below 0.55. The wordings *loose state* and *dense state* here are used in a relative sense and for ease of discussion. It is to some extent acceptable to use $e$ = 0.55 to categorize the specimens into two groups because no attempt has been made in this study to develop a function of mechanical properties (e.g., overall friction angle) on the basis of the void ratio and relative density. Table 1 gives the general information about the test series conducted, including the void ratios at different friction conditions.

In analyzing direct shear test data, the mobilized friction angle ($\phi_d$) is defined as

$$\tan\phi_d = \tau/\sigma \tag{1}$$

where $\tau$ and $\sigma$ = shear and normal stresses, respectively. On the basis of the vertical and horizontal displacements recorded during shearing, the dilation angle in direct shear ($\psi$) is defined as

$$\tan\psi = \delta v/\delta h \tag{2}$$

**Table 1.** Test Series Conducted

| Test material | Packing state | Interparticle friction condition | Particle size distribution | Normal pressure (kPa) | Initial void ratio |
|---|---|---|---|---|---|
| Glass beads | Loose | I | a, b, c, d | 19.6, 49.0, 78.4 | 0.56–0.69 |
| | | II | a, b, c, d | 19.6, 49.0, 78.4 | 0.61–0.69 |
| | | III | a, b, c, d | 19.6, 49.0, 78.4 | 0.55–0.64 |
| | | IV | a, b, c, d | 19.6, 49.0, 78.4 | 0.59–0.66 |
| | Dense | I | a, b, c, d | 19.6, 49.0, 78.4 | 0.44–0.55 |
| | | II | a, b, c, d | 19.6, 49.0, 78.4 | 0.50–0.55 |
| | | III | a, b, c, d | 19.6, 49.0, 78.4 | 0.47–0.54 |
| | | IV | a, b, c, d | 19.6, 49.0, 78.4 | 0.47–0.56 |

Note: I = dry state; II = water-lubricated; III = water-flooded; IV = oil-lubricated.



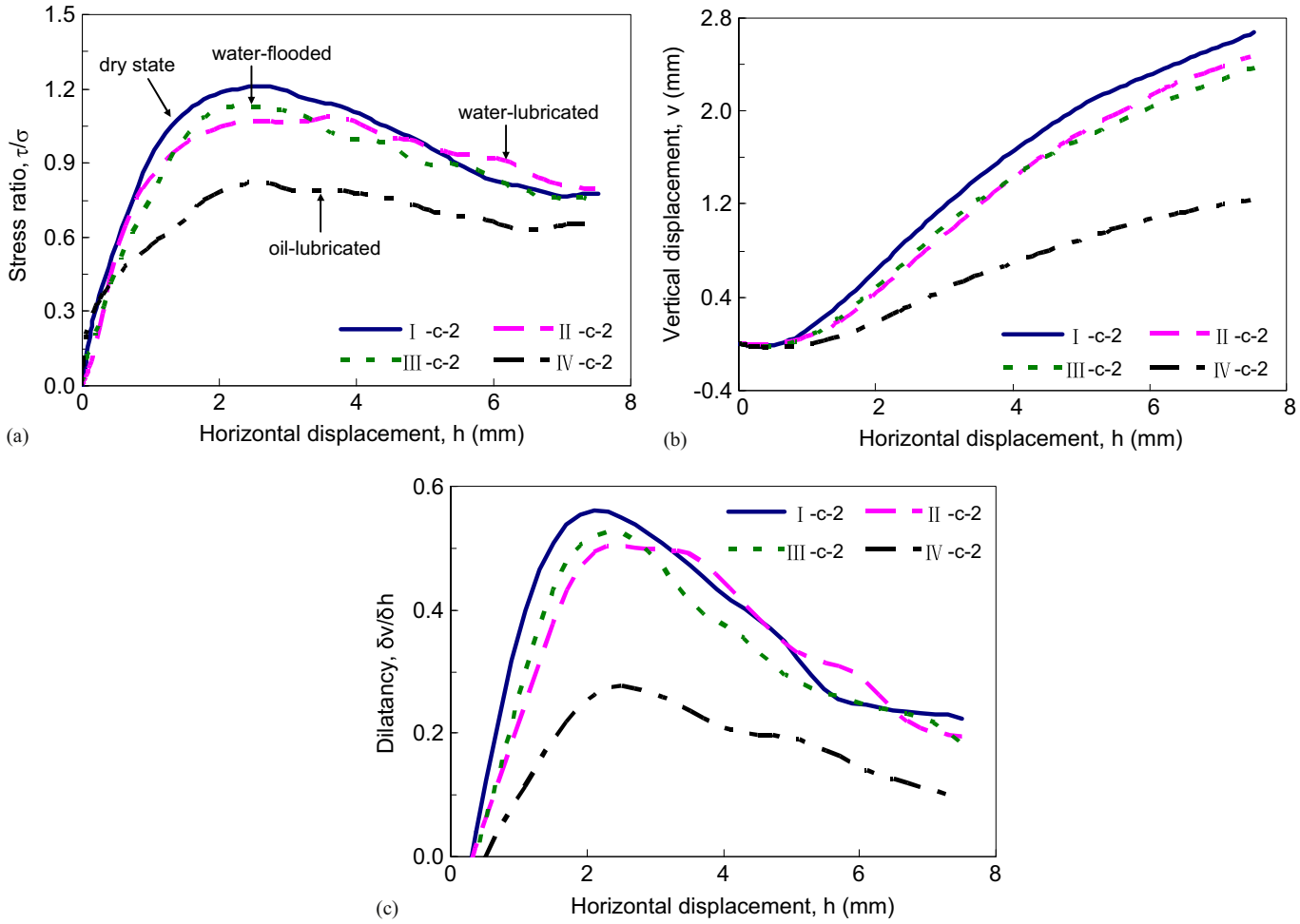


**Fig. 3.** Effect of interparticle friction on the shear response of glass beads of Gradation c (normal stress = 49.0 kPa): (a) stress ratio ($\tau/\sigma$) versus horizontal displacement ($h$); (b) vertical displacement ($v$) versus horizontal displacement ($h$); and (c) dilatancy ($\delta v/\delta h$) versus horizontal displacement ($h$)

where $\delta v$ and $\delta h$ = incremental vertical and horizontal displacements, respectively. The peak values of the mobilized friction angle and dilation angle are referred to as the peak friction angle $\phi_{max}$ and the peak dilation angle $\psi_{max}$.

## Shear Behavior and Shear Strength

### *Effect of Interparticle Friction Condition*

Fig. 3 shows shear responses of four specimens of glass beads having different interparticle friction conditions, where the plot in Fig. 3(a) is the variation of the stress ratio ($\tau/\sigma$) with the horizontal displacement, the plot in Fig. 3(b) is the vertical displacement versus the horizontal displacement, and the plot in Fig. 3(c) is the dilatancy ($\delta v/\delta h$) versus the horizontal displacement. The four specimens share the same particle gradation, same normal stress level (49.0 kPa), and similar initial void ratio ($e_{ini} = 0.50-0.54$). Therefore, the discrepancies observed in Fig. 3 can be mainly attributed to the influence of interparticle friction.

One of the significant observations is that the oil-lubricated glass beads exhibit a more contractive response when compared with the glass beads in dry, moisture, and flooded states. The overall shear behavior of the glass beads in moisture and flooded states do not show a notable difference from those in a dry state. This could be because a water film cannot effectively develop at

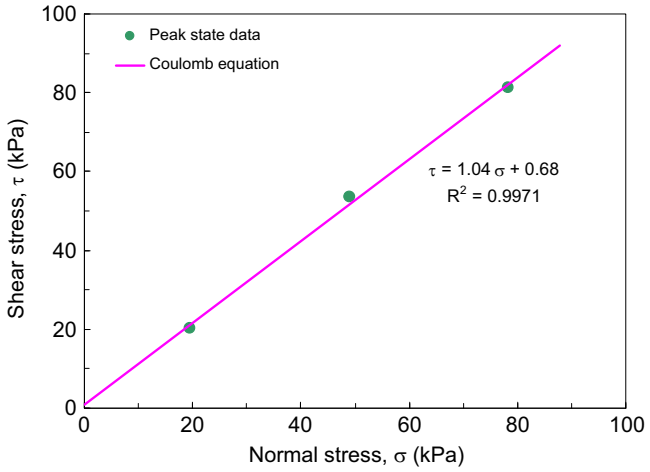


**Fig. 4.** Best fitting of the direct shear test data of three water-lubricated samples with Gradation d at the same initial void ratio ($e_{ini} = 0.50$)

**Table 2.** Values of Friction Angle and Dilation Angle at Peak State and Near-Constant-Volume State

| Test series | $e_{ini}$ | $\phi_{max}$ (degrees) | $\psi_{max}$ (degrees) | $\phi_{n\_cv}$ (degrees) | $\psi_{n\_cv}$ (degrees) |
|---|---|---|---|---|---|
| I-c-2 | 0.50 | 49.66 | 29.29 | 37.20 | 12.90 |
| II-c-2 | 0.53 | 46.43 | 26.65 | 38.28 | 11.29 |
| III-c-2 | 0.54 | 47.68 | 27.69 | 36.70 | 12.19 |
| IV-c-2 | 0.53 | 38.34 | 15.37 | 32.19 | 6.07 |
| I-d-2 | 0.56 | 30.02 | 5.48 | 27.75 | 2.95 |
| II-d-2 | 0.62 | 32.52 | 6.05 | 27.32 | 0.70 |
| III-d-2 | 0.59 | 34.14 | 8.42 | 28.37 | 2.57 |
| IV-d-2 | 0.60 | 21.62 | − 1.00 | 21.44 | − 1.49 |

the contact point between glass beads in a flooded state; also, no substantial matrix suction effect acts in a water-lubricated state. As can be seen in Fig. 4, the Coulomb equation obtained by best fitting the peak-stress data points of three water-lubricated specimens of Gradation d, which were sheared under different normal stresses but at the same initial void ratio ($e_{ini} = 0.50$), shows that the intercept is almost zero, indicating that the matrix suction exerts little effect.

Using Eq. (1), the values of the peak friction angle ($\phi_{max}$) were determined for the four specimens and summarized in Table 2. The three specimens in dry, moisture, and flooded states have somehow comparable values of $\phi_{max}$ (49.66°, 46.43°, and 47.68°), whereas the specimen of oil-lubricated glass beads has a markedly lower friction angle (38.34°). This finding is consistent with that of Skinner (1969), who reported that glass beads in dry and flooded states exhibited similar overall shear behavior and peak strength.

Furthermore, using Eq. (2), the values of peak dilation angle ($\psi_{max}$) were also determined for the four specimens, as summarized in Table 2. A similar trend can be seen that the oil-lubricated specimen has a significantly lower dilation angle compared with the other three specimens.

Fig. 3(c) shows that the dilatancy ($\delta v/\delta h$) at the end of the tests does not approach zero, implying that the constant-volume condition or the critical state was not achieved, even at large shear displacements. Nevertheless, the stress ratio ($\tau/\sigma$) in this final shearing stage tends to reach a stable value. For the glass beads in dry, moisture, and flooded states, this stable value is around 0.8, whereas for the oil-lubricated glass beads it is around 0.65. This suggests that there is a notable difference (~5.2°) in the friction angle mobilized at large shear displacements or at the near-constant-volume condition between the oil-lubricated specimen and the other three specimens with different interparticle friction. The maximum shear displacement in this study is around 7.5 mm, the ratio of which against the sample size (100 × 100 mm) is about 7.5/100 = 7.5%, obviously higher than the values in Jewell and Wroth (1987) (6/254 = 2.4%) and in Shibuya et al. (1997) (10/150 = 6.7%). It is thereby believed that the shear displacement in the current study is adequately large for the examination of the postpeak shear behavior.

Similar results and observations were obtained from another set of tests on glass beads of Gradation d, as shown in Fig. 5 and summarized in Table 2. The four tests provide consistent evidence that the interparticle friction introduced by oil lubrication can cause a significantly different shear behavior and shear strength, whereas the glass beads under the other three surface friction conditions (i.e., dry, water moisture, and flooded states) show a similar shear response and shear strength. A further discussion of the effect of interparticle friction on the friction angle at the constant-volume condition, $\phi_{cv}$ (i.e., the critical-state friction angle, $\phi_{cs}$) will be given later in the section on stress–dilatancy relations.

### *Effect of Mean Particle Size ($d_{50}$)*

Fig. 6 shows the shear responses of a set of specimens having different mean particle sizes but the same interparticle friction, subjected to the same normal stress of 19.6 kPa. Apparently, particle size has a notable effect on the overall shear response. For instance, Specimen II-c-1 ($e_{ini} = 0.54$; $d_{50} = 5.17$ mm) is packed at a similar void ratio as Specimen II-a-1 ($e_{ini} = 0.56$; $d_{50} = 2.22$ mm), but the former behaves in a more dilative manner than the latter. The peak stress ratio and the value of dilatancy for the Specimen II-c-1 were determined to be 1.381 and 0.557, being markedly higher than that for Specimen II-a-1: 0.819 and 0.345. The observed discrepancies can mainly be attributed to the difference in mean particle size ($d_{50}$) as the two specimens have a similar coefficient of uniformity, similar interparticle friction condition and similar packing density.

The size effect can also be observed on Specimens II-b-1 and II-c-1 shown in the same plots. Consistent observations have been obtained on another pair of specimens (II-a-3 and II-b-3) as shown in Fig. 7, both having a similar void ratio (~0.50) and being subjected to the same normal stress (78.4 kPa).

Again, the plots in Figs. 6(c) and 7(c) show that the dilatancy at large shear displacements is not zero, implying that the critical state was not yet reached at the end of the tests. Nevertheless, given the evolutions of the stress ratio and dilatancy in the final stage of shearing, it is reasonable to infer that mobilization of the critical state should be related to particle size. To verify this, the relations of the near-constant-volume friction angle ($\phi_{n\_cv}$) and the corresponding dilation angle ($\psi_{n\_cv}$) with mean particle size $d_{50}$ are examined with the relevant test data, as shown in Fig. 8. For brevity, the letters *L* and *D* in the legends stand for loose and dense packing states, respectively (see Table 1). Both $\phi_{n\_cv}$ and $\psi_{n\_cv}$ show a fairly good correlation with mean particle size ($d_{50}$) in that they both increase with $d_{50}$.

## Stress–Dilatancy Relations

The stress–dilatancy relation plays an important role in studying the shear behavior of granular materials. For specimens of dry and

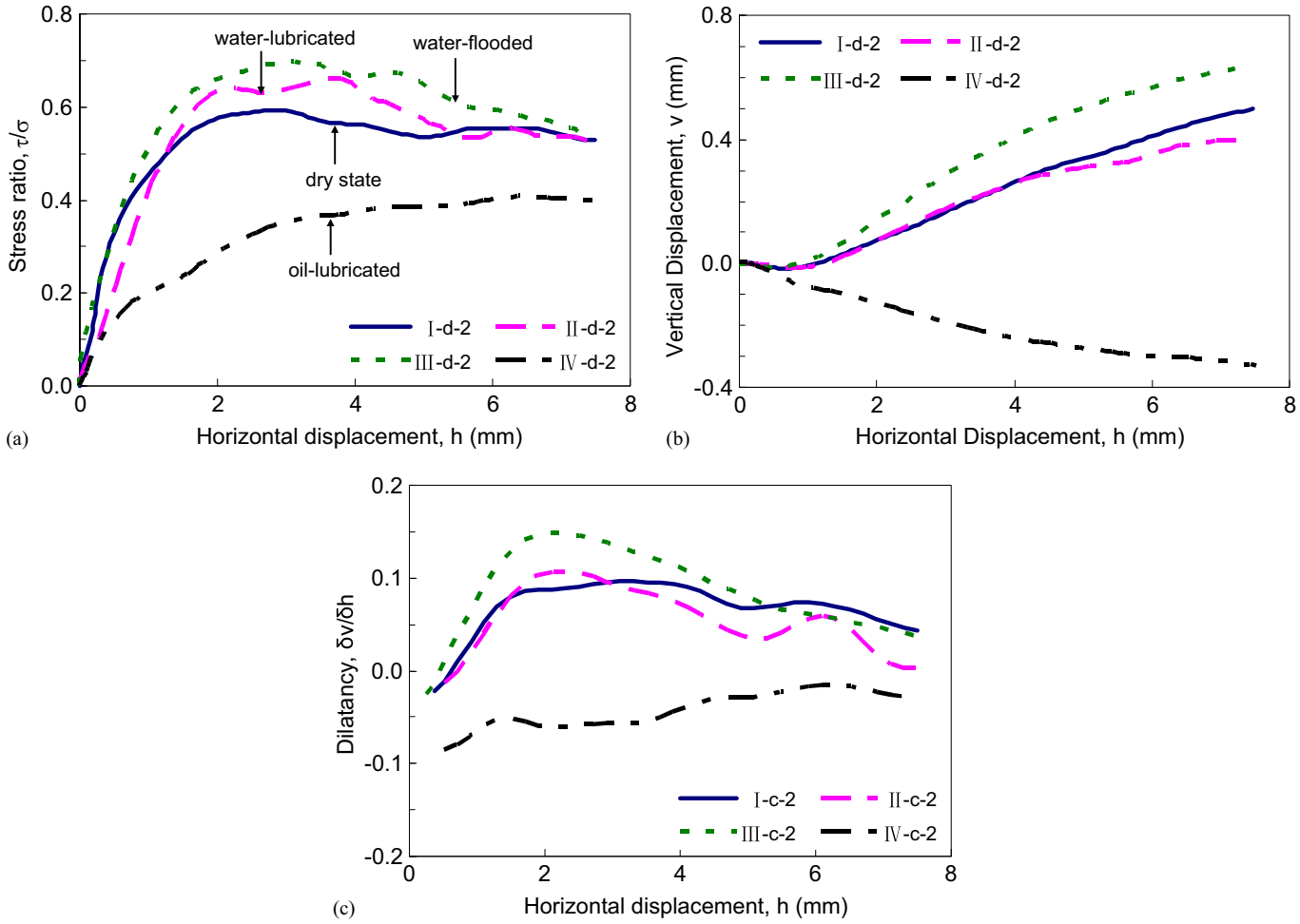


**Fig. 5.** Effect of interparticle friction on the shear response of glass beads of Gradation d (normal stress = 49.0 kPa): (a) stress ratio ($\tau/\sigma$) versus horizontal displacement ($h$); (b) vertical displacement ($v$) versus horizontal displacement ($h$); and (c) dilatancy ($\delta v/\delta h$) versus horizontal displacement ($h$)

oil-lubricated glass beads with different gradations, the mobilized friction angle defined in Eq. (1) was determined and plotted in Fig. 9 against the dilation angle defined in Eq. (2), with the use of test data at the shear displacements of 2.0, 3.0, 4.0, 5.0, and 6.0 mm and at the peak state. The trend lines in these plots are the best-fitting lines for the data points. The intercepts of these trend lines give the values of the critical-state friction angle $\phi_{cs}$ (i.e., constant-volume friction angle, $\phi_{cv}$), whereas the slopes of these lines give the values of the dilatancy coefficient, denoted here as $\varsigma$.

It is evident from Fig. 9 that the stress–dilatancy relation is dependent on the interparticle friction condition and particle size. In other words, both the critical-state friction angle $\phi_{cs}$ and the dilatancy coefficient $\varsigma$ are found to depend on these two factors. For clarity, a summary of the values of $\phi_{cs}$ and $\varsigma$ for the various testing conditions is given in Table 3.

An alternative view of this dependence is given in Fig. 10, where the values of $\phi_{cs}$ and $\varsigma$ at different gradations and interparticle friction conditions are compared. Among the four interparticle friction conditions, oil lubrication always leads to the smallest values of $\phi_{cs}$ regardless of gradation [see Fig. 10(a)]. The interparticle friction conditions in terms of dry, water-lubricated, and water-flooded states, however, do not make a big difference in $\phi_{cs}$. For example, in the case of particle Gradation a, the value of $\phi_{cs}$ under oil lubrication was determined to be 20.8°, whereas the values of $\phi_{cs}$ under the other three interparticle friction conditions were markedly higher, being 25.0°, 27.3°, and 25.3°, respectively. However, these angle values may not be comparable to the angle of repose for glass beads. This is because the angle of repose relies not only on the interparticle friction condition, but also on the boundary condition in the experiments.

Similarly, the average value of $\varsigma$ under oil lubrication was determined to be 0.98 for the four types of gradations, being significantly larger than average $\varsigma$ values determined for the cases of dry, water-lubricated, and water-flooded states ($\varsigma = 0.67$, 0.66, and 0.75, respectively).

The experimental data in Fig. 9 suggest that the stress–dilatancy relation takes a general form as

$$\phi_d = \varsigma \cdot \psi + \phi_{cs} \tag{3}$$

in which $\phi_d$ = mobilized friction angle, and $\varsigma$ = dilatancy coefficient that will vary with the interparticle friction and particle size [it will range between 0.59 and 1.02 for the tests conducted (see Table 3)]. Obviously, the classic stress–dilatancy relation established using the idealized saw-tooth model or the work-energy principle for direct shear tests on Ottawa standard sand (Wood 1990; Taylor 1948), as given in the following equation, can be regarded as a special case of the generalized relation in that the dilatancy coefficient $\varsigma$ is taken as unity

$$\phi_d = \psi + \phi_{cs} \tag{4}$$

Bolton (1986) proposed a modified stress–dilatancy relation based on an analysis of a database of plane-strain and triaxial tests

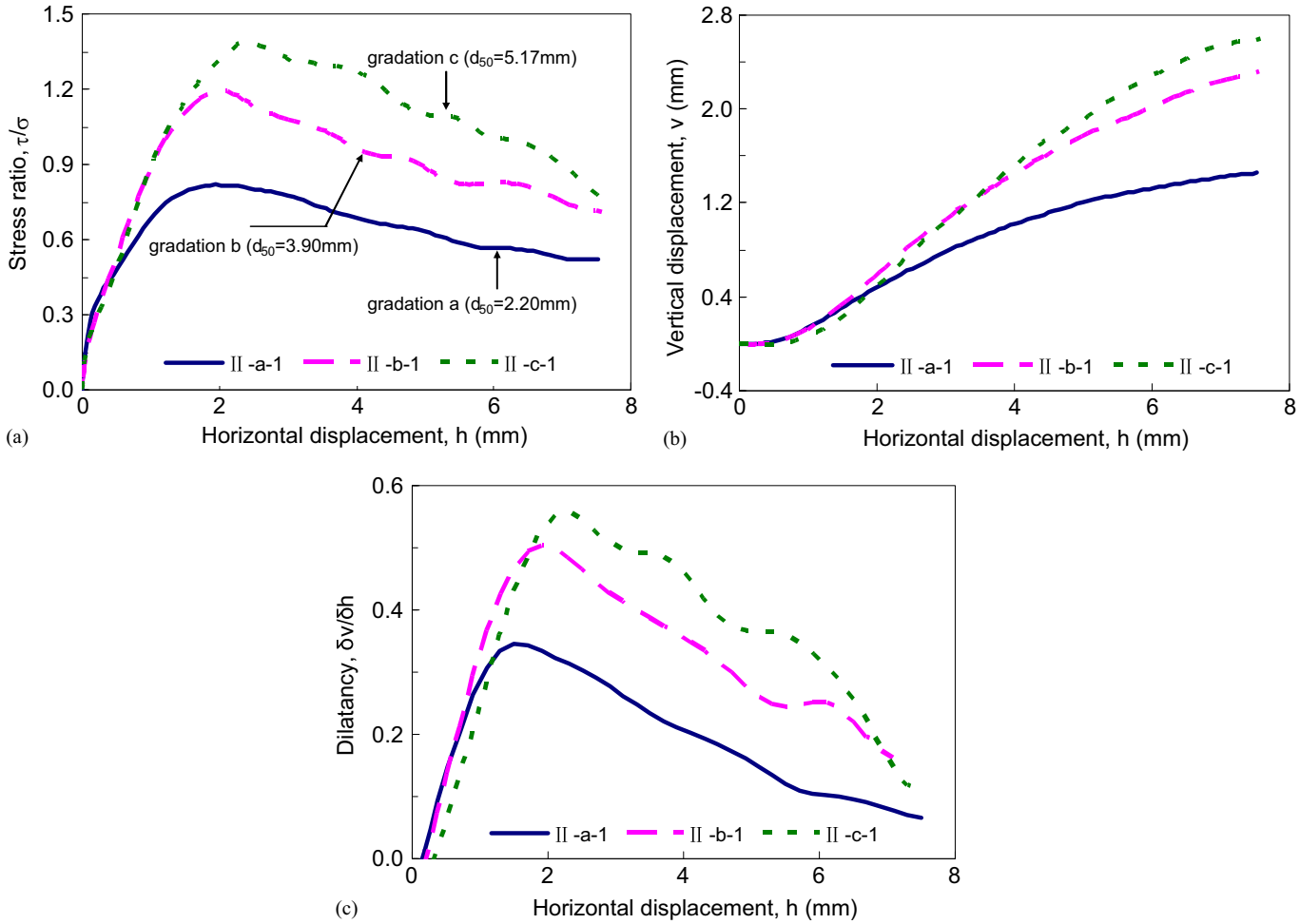


**Fig. 6.** Effect of particle size on the shear response of water-lubricated glass beads (normal stress = 19.6 kPa): (a) stress ratio ($\tau/\sigma$) versus horizontal displacement ($h$); (b) vertical displacement ($v$) versus horizontal displacement ($h$); and (c) dilatancy ($\delta v/\delta h$) versus horizontal displacement ($h$)

on sands as follows:

$$\phi_d = 0.8\psi + \phi_{cs} \tag{5}$$

Apparently, Bolton's stress–dilatancy relation is also a special case, with the dilatancy coefficient being 0.8.

For the purpose of comparison, Fig. 11 shows the generalized stress–dilatancy relation in terms of $(\varsigma \cdot \psi)$ versus $(\phi_d - \phi_{cs})$ for a variety of $\varsigma$ values determined from the direct shear tests in the present study, together with the two classic stress–dilatancy relations. Taylor's relation is approximately an upper bound, whereas Bolton's relation approximately represents an average. Following are several possible reasons why a variable $\varsigma$ was not observed in Bolton's work:

1. Most of the sands in the database compiled by Bolton (1986) are saturated quartz sands, and their interparticle friction conditions do not differ considerably from one another. As a result, the effect of surface friction on the stress–dilatancy relation cannot be reflected by the database.
2. The sands in the database show a large discrepancy in mean particle size from the test materials in the present study. The average particle sizes of the sands fall into a narrow range from 0.1 to 0.8 mm, whereas the mean sizes of the test materials in the present study are in the range of 2.2 to 5.2 mm. The effects of particle size may not be adequately reflected by the database of sands.

## Micromechanical Considerations

Different particle–surface friction conditions should indicate different interparticle friction angles ($\phi_\mu$). It remains a challenge to accurately measure the values of $\phi_\mu$ in the laboratory. Here, an attempt is made to approximately estimate the range of $\phi_\mu$ for the four surface-friction conditions, based on a published database for particle–surface friction (Tribology 2013; Rowe 1971). As summarized in Table 4, the value of $\phi_\mu$ for oil-lubricated glass beads varies from approximately 6° to 17°, whereas the range of $\phi_\mu$ for dry glass beads is between 15° and 25°. For water-flooded glass beads, the value of $\phi_\mu$ is estimated to range from about 20° to 30°, whereas for water-lubricated glass beads, the value of $\phi_\mu$ is slightly larger (22–32°) to take into account the possible effect of capillary forces (Gabrieli et al. 2012).

Given the estimated $\phi_\mu$ values and the values of $\phi_{cv}$ determined from the tests, the data points are superimposed onto Fig. 1. It can be seen that the new data confirm the variation trend manifested by the digital elevation model simulations. In particular, $\phi_{cv}$ does not show a considerable variation with $\phi_\mu$ when $\phi_\mu$ is beyond some threshold value (10–15°), and when $\phi_\mu$ is less than this threshold value, $\phi_{cv}$ tends to increase with $\phi_\mu$. This trend would not be affected even $\phi_\mu$ takes a reasonably wide range of values to account for the uncertainty in laboratory measurements. The possible mechanism for this trend is considered as follows. In the low $\phi_\mu$ region, particle sliding tends to be dominant such that $\phi_{cv}$



Int. J. Geomech., 2016, 16(1): 04015011

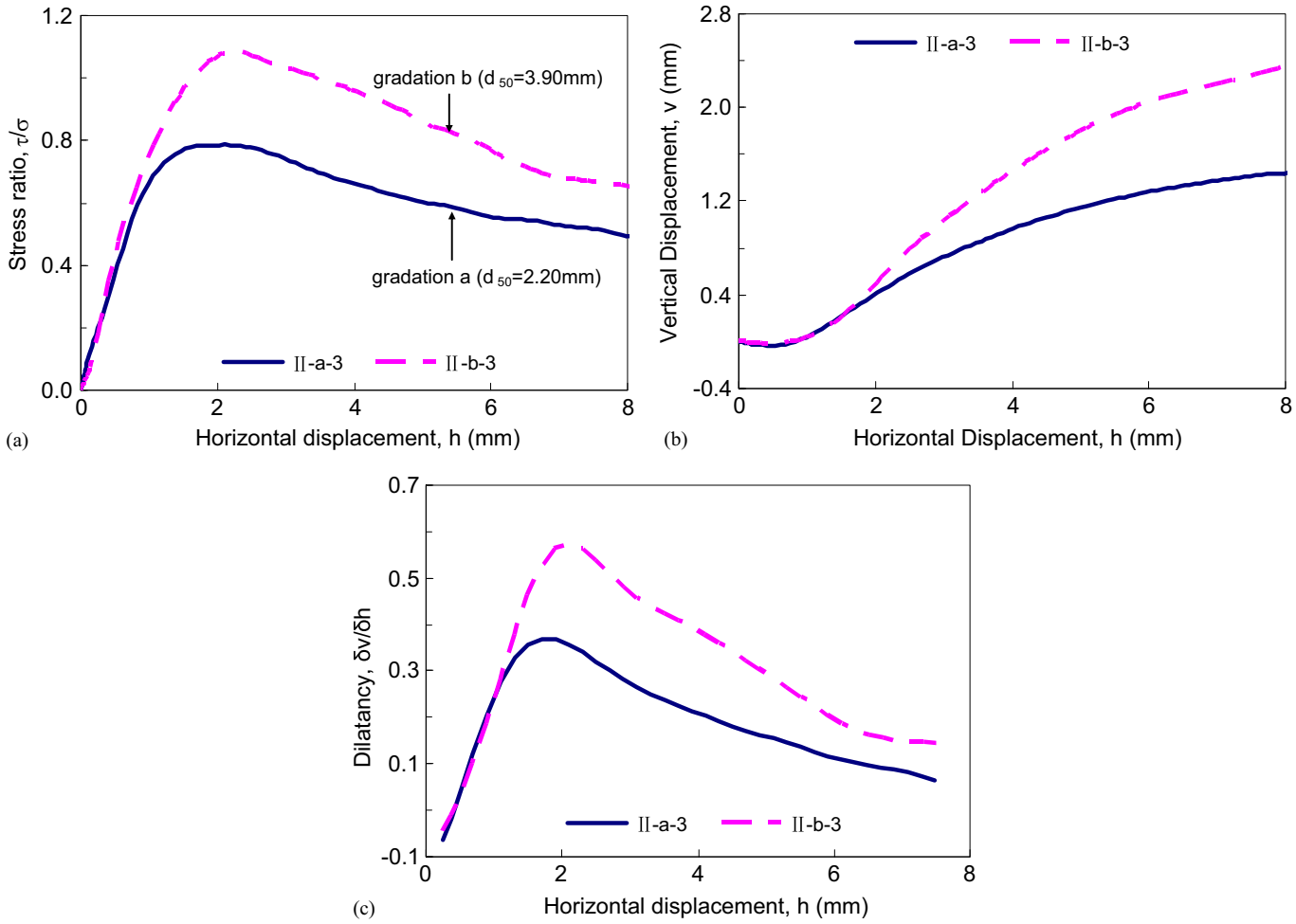


**Fig. 7.** Effect of particle size on the shear response of water-lubricated glass beads (normal stress = 78.4 kPa): (a) stress ratio ($\tau/\sigma$) versus horizontal displacement ($h$); (b) vertical displacement ($v$) versus horizontal displacement ($h$); and (c) dilatancy ($\delta v/\delta h$) versus horizontal displacement ($h$)

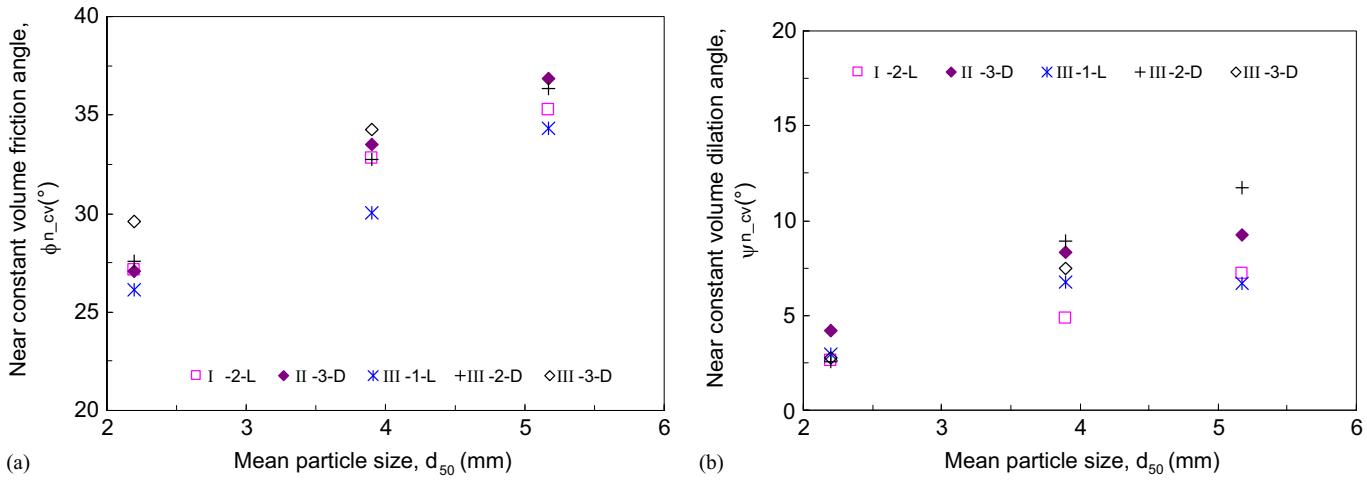


**Fig. 8.** Variations of (a) the near constant-volume friction angle and (b) the near constant-volume dilation angle with mean particle size

increases with an increase in $\phi_\mu$. As $\phi_\mu$ continues to increase, the difficulty for particles to slide against one another becomes larger, and particle rolling tends to play a more important role. In other words, as $\phi_\mu$ keeps increasing, the chance for particle sliding is reduced, but the chance for particle rolling is promoted. The interparticle rolling friction coefficient is far smaller than the interparticle sliding friction coefficient. As a result, these two types of particle movements tend to reach a balance at some threshold value of $\phi_\mu$ such that $\phi_{cv}$ does not show a significant variation with a further increase of $\phi_\mu$.

Dilatancy is assumed to be caused by the variation of the void area (volume) within a specific specimen under shear, and the variation of the void area (volume) may lead to the change of void ratio, as well. The particle size is thereby supposed to play



Int. J. Geomech., 2016, 16(1): 04015011

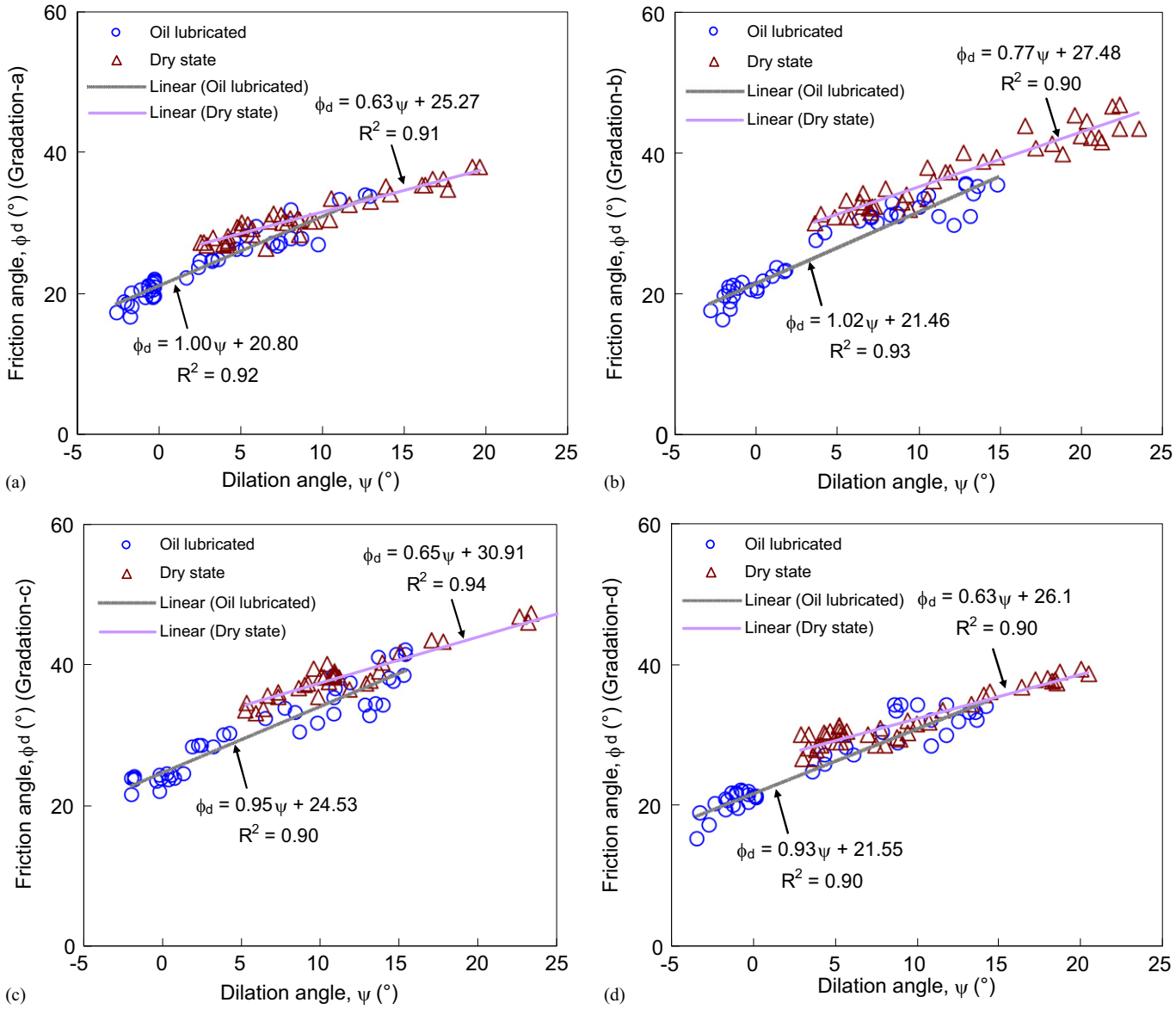


**Fig. 9.** Mobilized friction angle versus dilation angle: (a) Gradation a; (b) Gradation b; (c) Gradation c; and (d) Gradation d

**Table 3.** Values of Dilatancy Coefficient $\varsigma$ and Constant-Volume Friction Angle $\phi_{cv}$

| Interparticle friction condition | Particle size distribution | $\varsigma$ | $\phi_{cv}$ (degrees) | $R^2$ |
|---|---|---|---|---|
| I | a | 0.63 | 25.27 | 0.91 |
| | b | 0.77 | 27.48 | 0.90 |
| | c | 0.65 | 30.91 | 0.94 |
| | d | 0.63 | 26.10 | 0.90 |
| II | a | 0.59 | 27.27 | 0.73 |
| | b | 0.63 | 29.95 | 0.91 |
| | c | 0.66 | 30.96 | 0.90 |
| | d | 0.76 | 27.67 | 0.95 |
| III | a | 0.79 | 25.02 | 0.85 |
| | b | 0.70 | 28.44 | 0.77 |
| | c | 0.78 | 27.19 | 0.87 |
| | d | 0.74 | 28.12 | 0.88 |
| IV | a | 1.00 | 20.80 | 0.92 |
| | b | 1.02 | 21.46 | 0.93 |
| | c | 0.95 | 24.53 | 0.90 |
| | d | 0.93 | 21.55 | 0.90 |

a role in the variation of the void area (volume) and void ratio, as well as dilatancy. A conceptual model is proposed in Fig. 12 to explain the observed size effect on dilatancy. Initially, the assembly of four spheres of radius $r$ is packed in a dense state; after shearing it dilates with the void area being increased by $(4-2\sqrt{3})r^2$. This proves that the volume change or the dilatancy depends on the particle size. The void ratio of the two-dimensional (2D) conceptual model in Fig. 12 is different from a real three-dimensional (3D) packing pattern, and it is thus difficult to justify the void ratio of real 3D packing by identifying the theoretical maximum and minimum void ratios of this 2D conceptual model. This, however, does not affect the findings based on the experimental observations.

As discussed in the preceding section, under otherwise similar testing conditions, the friction angle at critical state, $\phi_{cs}$, tends to increase with mean particle size $d_{50}$. To explain this effect, a conceptual model is given in Figs. 13(a and b), where Particle 1 with the radius $r_1$ is in contact with Particle 2 of radius $r_2$. Under the normal force $\Delta N$ and the shear force $\Delta S$, Particle 1 slides against Particle 2 from Point $c$ to Point $c'$, and the sliding path on



Int. J. Geomech., 2016, 16(1): 04015011

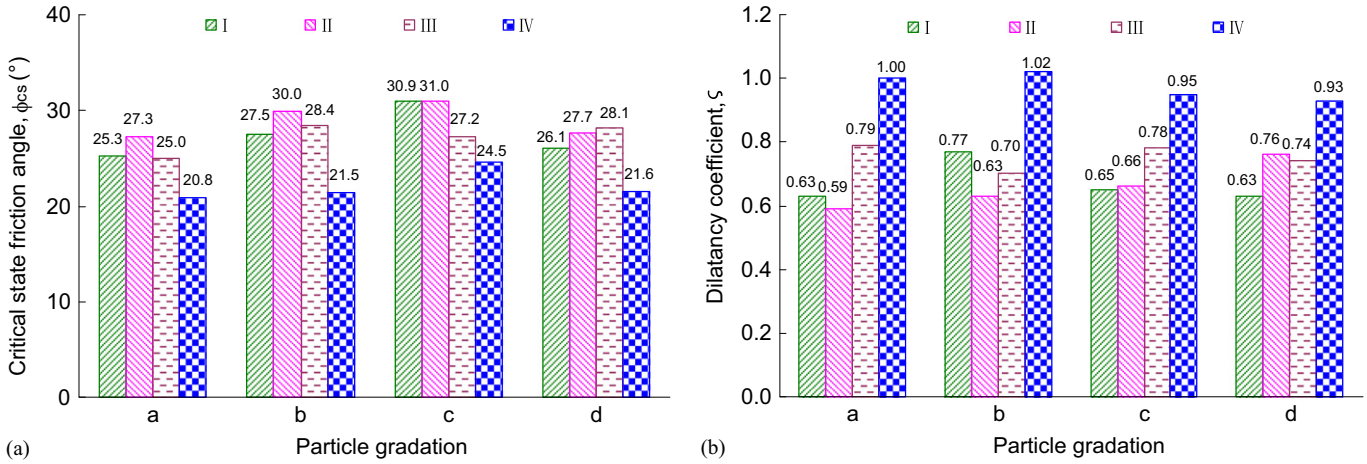


**Fig. 10.** Dependence of (a) critical-state friction angle and (b) dilatancy coefficient on the interparticle friction condition for glass beads of different particle gradations

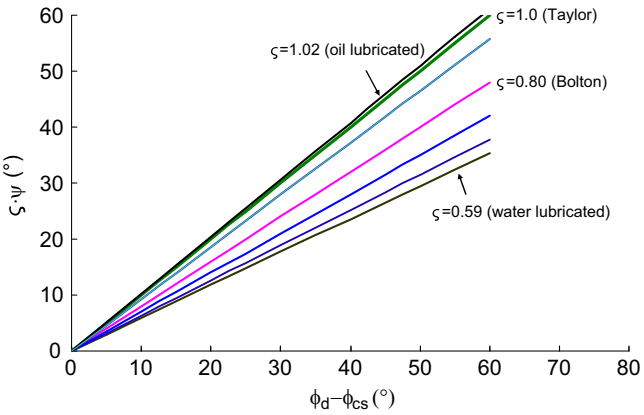


**Fig. 11.** The relation between $(\varsigma \cdot \psi)$ and $(\phi_d - \phi_{cs})$ for various values of dilatancy coefficient

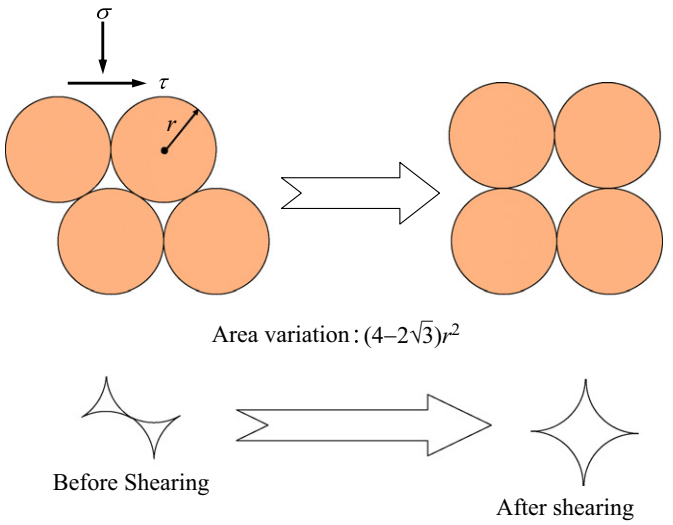


**Fig. 12.** Conceptual model for explanation of the observed effect of particle size on dilatancy

**Table 4.** Estimated Range of Interparticle Friction Angle

| Interparticle friction condition | Interparticle friction angle (degrees) | | |
|---|---|---|---|
| | $(\phi_\mu)_{\min}$ | $(\phi_\mu)_{\max}$ | $(\phi_\mu)_{ave}$ |
| I | 10 | 25 | 17.5 |
| II | 22 | 32 | 27 |
| III | 20 | 30 | 25 |
| IV | 6 | 16 | 11 |

Note: $(\phi_\mu)_{ave}$ is the mean value.

Particle 2, namely, arc $cc'$, is symmetrical about the axis such that no volume change occurs. The work done by the shear force $\Delta S$ during the sliding process can then be given as follows:

$$W_S = \int \Delta f dL \tag{6}$$

where $\Delta f =$ friction force between particles; $dL =$ incremental relative displacement between particles at a very small angle increment $d\alpha$ as shown in Fig. 13(c). Given this microscopic sliding model, it is assumed that the Particle 1 slides against Particle 2 with the forces exerting on Particle 1 being balanced. During the sliding process, the acute angle formed between the tangential contact plane and the horizontal plane, as indicated by Fig. 14(a), is noted as $\gamma$. Equilibrium equations can be thus established in the vertical direction for Particle 1 at the two representative sliding states, as shown in Figs. 14(b and c), and they are written as

$$\Delta f_L \sin\gamma - \Delta P \cos\gamma + \Delta N = 0 \quad \text{[for the state in Fig. 14(b)]} \tag{7}$$

$$\Delta f_R \sin\gamma + \Delta P \cos\gamma - \Delta N = 0 \quad \text{[for the sliding state in Fig. 14(c)]} \tag{8}$$

where $\Delta f_L$ and $\Delta f_R =$ friction forces at these two sliding states, and $\Delta P =$ normal contact force. The friction force can be expressed to be $\Delta P \tan\phi_\mu$, where $\phi_\mu$ is the interparticle (sliding) friction angle. The friction forces $\Delta f_L$ and $\Delta f_R$ are therefore derived to be

$$\Delta f_L = \frac{\tan\phi_\mu \Delta N}{\cos\gamma - \tan\phi_\mu \sin\gamma} \tag{9}$$

$$\Delta f_R = \frac{\tan\phi_\mu \Delta N}{\cos\gamma + \tan\phi_\mu \sin\gamma} \tag{10}$$

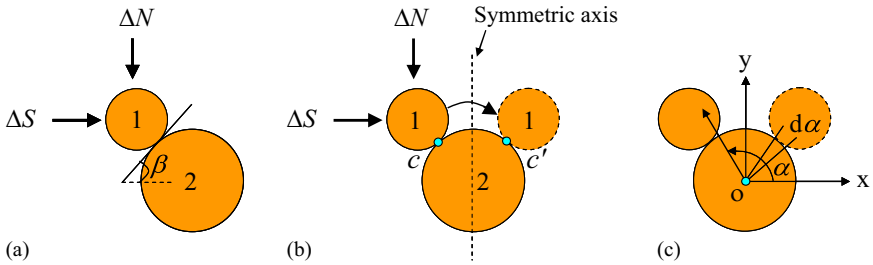


**Fig. 13.** Conceptual model for explanation of the observed effect of particle size on the critical state friction angle: (a) initial state; (b) sliding process; and (c) reference coordinate system

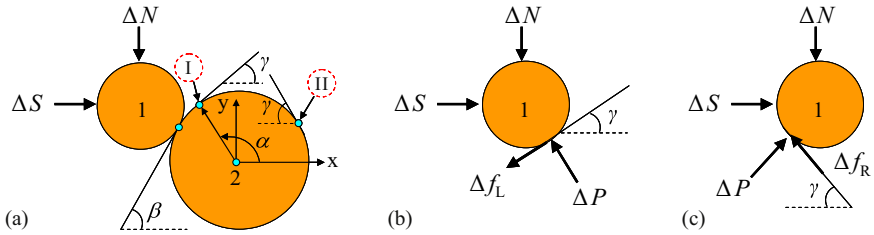


**Fig. 14.** Representation of (a) the angle $\gamma$ at the two Sliding States I and II; (b) the force condition at Sliding State I; and (c) the force condition at Sliding State II

In Fig. 14(a), such geometric relationships can be established between the angle $\gamma$ and the angle $\alpha$:

$$\gamma = \frac{\pi}{2} - \alpha \left(\alpha \le \frac{\pi}{2}\right) \tag{11}$$

$$\gamma = \alpha - \frac{\pi}{2} \left(\alpha > \frac{\pi}{2}\right) \tag{12}$$

With the geometric relations in Eqs. (11) and (12), the friction forces $\Delta f_L$ and $\Delta f_R$ in Eqs. (9) and (10) are unified to be

$$\Delta f = \Delta f_L = \Delta f_R = \frac{\tan\phi_\mu \Delta N}{\sin\alpha + \tan\phi_\mu \cos\alpha} \tag{13}$$

The value of $dL$ can be expressed as

$$dL = (r_1 + r_2)d\alpha \tag{14}$$

With Eqs. (13) and (14), Eq. (6) is transformed to be

$$W_S = \int_{\pi/2-\beta}^{\pi/2+\beta} \frac{\tan\phi_\mu \Delta N}{\sin\alpha + \tan\phi_\mu \cos\alpha}(r_1 + r_2)d\alpha \tag{15}$$

where $\beta =$ orientation angle of the tangential contact plane at the initial point of the sliding path. The integration result of the Eq. (15) is finally given to be

$$W_S = \Delta N(r_1 + r_2)\sin\phi_\mu \ln\left[\frac{\tan\left(\frac{\pi}{4} + \frac{\beta}{2} + \frac{\phi_\mu}{2}\right)}{\tan\left(\frac{\pi}{4} - \frac{\beta}{2} + \frac{\phi_\mu}{2}\right)}\right] \tag{16}$$

It follows from Eq. (16) that the work done by the shear force $\Delta S$ is proportional to the summation of $r_1$ and $r_2$. That means the larger the particle size is, the greater the work needed to overcome the frictional resistance. Following the derivation steps above, a similar work-energy equation can be obtained for the particle-rolling behavior, with the interparticle sliding friction angle $\phi_\mu$ in Eq. (16) replaced to be the interparticle rolling friction angle $\phi_r$. From this point of view, the overall friction angle is expected to increase with increasing particle size.

## Conclusions

Diverse or even contradictory views exist in the literature on the effects of interparticle friction and particle size on the mechanical behavior of granular materials. A series of direct shear tests have been conducted on glass beads of varying sizes and surface friction levels to address this issue. The main results and observations of this study are summarized as follows:

1. Under otherwise similar testing conditions, the overall shear response and shear strength of the glass beads in water-lubricated and water-flooded states appeared to be similar to that of the glass beads in a dry state. Oil-lubricated glass beads, however, behaved in a significantly different manner, in that they were more contractive and exhibited markedly lower shear strength.
2. Particle size may affect the shear behavior and shear strength of granular materials. Under otherwise similar testing conditions, glass beads with a larger mean particle size ($d_{50}$) exhibited a more dilative shear response; both the peak friction angle and the near-constant-volume friction angle tended to increase with increasing mean particle size.
3. The relationship between the mobilized friction angle and the dilation angle is affected by the interparticle friction condition and particle size. A generalized stress–dilatancy relation is proposed by introducing a dilatancy coefficient that varies with interparticle friction and particle size. The experimental data indicate that the dilatancy coefficient ranges from 0.59 to 1.02. However, in the classic stress–dilatancy relations, the dilatancy coefficient is treated as a constant (0.8 or 1).
4. With respect to the relationship between the constant-volume friction angle ($\phi_{cv}$) and the interparticle friction angle ($\phi_\mu$), it is postulated that particle sliding is a dominant mechanism when $\phi_\mu$ is below a transition value (10–15°). When $\phi_\mu$ is well

beyond this transition value, particle rolling may become dominant, leading to the experimental and numerical observation that $\phi_{cv}$ does not alter sensibly with $\phi_{\mu}$.

5. The work equation derived using an idealized microscopic model of particle sliding at the critical state suggests that the work done by the shear force to overcome the frictional resistance increases as the particle size increases, explaining the observation that the critical-state friction angle increases with mean particle size.

## Acknowledgments

This work was supported by the University of Hong Kong under the Seed Funding for Basic Research Scheme. The authors also want to thank the financial support provided by the National Natural Science Foundation of China under Grant Nos. 51209237, 51428901, and 41030747.

## Notation

*The following symbols are used in this paper*:

$d_{50}$ = mean particle size;
$e_{ini}$ = initial void ratio;
$\sigma$ = normal stress on the shear plane;
$\tau$ = shear stress along the shear plane;
$\varsigma$ = dilatancy coefficient;
$\phi$ = friction angle;
$\phi_{cv}$ = constant-volume friction angle;
$\phi_{cs}$ = critical-state friction angle;
$\phi_d$ = friction angle in the direct shear test;
$\phi_{\max}$ = peak friction angle;
$\phi_{n\_cv}$ = near-constant-volume friction angle;
$\phi_r$ = interparticle rolling friction angle;
$\phi_{\mu}$ = interparticle sliding friction angle;
$\psi$ = dilation angle in the direct shear test;
$\psi_{\max}$ = peak dilation angle; and
$\psi_{n\_cv}$ = near-constant-volume dilation angle.

## References

Al-Hussaini, M. (1983). "Effect of particle size and strain conditions on the shear strength of crushed basalt." *Can. Geotech. J.*, 20(4), 706–717.

Bishop, A. W. (1954). "Correspondence on shear characteristics of a saturated silt, measured in triaxial compression." *Géotechnique*, 4(1), 43–45.

Bolton, M. D. (1986). "The strength and dilatancy of sands." *Géotechnique*, 36(1), 65–78.

Caquot, A. (1934). *Equilibre des massifs à frottement interne*, Gauthier-Villars, Paris (in French).

Cavarretta, I., Coop, M., and O'Sullivan, C. (2010). "The influence of particle characteristics on the behaviour of coarse grained soils." *Géotechnique*, 60(6), 413–423.

Dai, B. B. (2010). "Micromechanical investigation of the behavior of granular materials." Ph.D. dissertation, Dept. of Civil Engineering, Univ. of Hong Kong, Hong Kong.

Gabrieli, F., Lambert, P., Cola, S., and Calvetti, F. (2012). "Micromechanical modelling of erosion due to evaporation in a partially wet granular slope." *Int. J. Numer. Anal. Meth. Geomech.*, 36(7), 918–943.

Hamidi, A., Azini, B., and Masoudi, C. (2012). "Impact of gradation on the shear strength-dilation behavior of well graded sand-gravel mixtures." *Sci. Iran. A*, 19(3), 393–402.

Horne, M. R. (1969). "The behaviour of an assembly of rotund, rigid, cohesionless particles. III." *Proc. R. Soc. London Ser. A*, 310(1500), 21–34.

Jaafar, R., and Likos, W. J. (2011). "Estimating water retention characteristics of sands from grain size distribution using idealized packing conditions." *Geotech. Test. J.*, 34(5), 1–14.

Jewell, R. A., and Wroth, C. P. (1987). "Direct shear tests on reinforced sand." *Géotechnique*, 37(1), 53–68.

Kruyt, N. P., and Rothenburg, L. (2006). "Shear strength, dilatancy, energy and dissipation in quasi-static deformation of granular materials." *J. Stat. Mech.: Theory Exp.* 7(paper no. P070210), 1–13.

Li, X., and Yu, H. (2013). "Particle-scale insight into deformation non-coaxiality of granular materials." *Int. J. Geomech.*, 10.1061/(ASCE)GM.1943-5622.0000338, 04014061.

Maeda, K., Hirabayashi, H., and Ohmura, A. (2006). "Micromechanical influence of grain properties on deformation-failure behavior of granular media by DEM." *Geomechanics and Geotechnics of Particulate Media*, M. Hyodo, H. Murata, and Y. Nakata, eds., Taylor & Francis, U.K., 173–180.

Mahmud Sazzad, M., Suzuki, K., and Modaressi-Farahmand-Razavi, A. (2012). "Macro-micro responses of granular materials under different *b* values using DEM." *Int. J. Geomech.*, 12(3), 220–228.

Marachi, N. D., Chan, C. K., and Seed, H. B. (1972). "Evaluation of properties of rockfill materials." *J. Soil Mech.*, 98(SM1), 95–112.

Ogbonnaya, I., Kyoji, S., and Hiroshi, S. (2009). "The geotechnical properties of sands with varying grading in a stress-controlled ring shear tests." *Electron. J. Geotech. Eng.*, 14(Bundle N), 1–21.

Oger, L., Savage, S. B., Corriveau, D., and Sayed, M. (1998). "Yield and deformation of an assembly of disks subjected to a deviatoric stress loading." *Mech. Mater.*, 27(4), 189–210.

O'Sullivan, C., Bray, J. D., and Riemer, M. F. (2002). "Influence of particle shape and surface friction variability on response of rod-shaped particulate media." *J. Eng. Mech.*, 10.1061/(ASCE)0733-9399(2002)128:11(1182), 1182–1192.

Oztoprak, S., and Bolton, M. D. (2013). "Stiffness of sands through a laboratory test database." *Géotechnique*, 63(1), 54–70.

Rowe, P. W. (1971). "Theoretical meaning and observed values of deformation parameters for soil." *Proc., Roscoe Memorial Symp.*, Foulis & Co., Cambridge, 143–194.

Shibuya, S., Mitachi, T., and Tamate, S. (1997). "Interpretation of direct shear box testing of sands as quasi-simple shear." *Géotechnique*, 47(4), 769–790.

Skinner, A. E. (1969). "A note on the influence of interparticle friction on the shear strength of a random assembly of spherical particles." *Géotechnique*, 19(1), 150–157.

Soria-Hoyo, C., Valverde, J. M., and Castellanos, A. (2009). "Avalanches in moistened beds of glass beads." *Powder Technol.*, 196(3), 257–262.

Suiker, A. S. J., and Fleck, N. A. (2004). "Frictional collapse of granular media." *J. Appl. Mech.*, 71(3), 350–358.

Taylor, D. W. (1948). *Fundamentals of soil mechanics*, John Wiley, New York.

Thornton, C. (2000). "Numerical simulations of deviatoric shear deformation of granular media." *Géotechnique*, 47(2), 319–329.

Tribology. (2013). "ROYMECH" ⟨http://www.roymech.co.uk/Useful_Tables/Tribology/co_of_frict.htm⟩ (Jan. 17, 2013).

Wood, D. M. (1990). *Soil behaviour and critical state soil mechanics*, Cambridge University Press, Cambridge, U.K.

Yang, J., and Wei, L. M. (2012). "Collapse of loose sand with the addition of fines: The role of particle shape." *Géotechnique*, 62(12), 1111–1125.